Asian Journal of Chemistry; Vol. 36, No. 6 (2024), 1371-1376

ASIAN JOURNAL OF CHEMISTRY

https://doi.org/10.14233/ajchem.2024.31405

Carboxamide-based Fluorescent Sensor for the Detection of Mg^{2+} and Ni^{2+} Ions

NETRA PAL SINGH[1,†,*], MAITREYI SINGH[1], ANAND RATNAM[1] and ANUROOP KUMAR[2]

[1]Department of Chemistry, D.D.U. Gorakhpur University, Gorakhpur-273009, India
[2]Department of Chemistry, Meerut College, Meerut-250003, India
[†]Present address: Department of Chemistry, Dr. H.S. Gour Vishwavidyalaya (A Central University), Sagar-470003, India

*Corresponding author: E-mail: npsmcm.in@gmail.com

Received: 14 February 2024; *Accepted*: 30 April 2024; *Published online*: 31 May 2024; AJC-21651

In this work, pyridine-2,6-dicarboxamide based ligand was synthesized by reacting pyridine-2,6-dicarboxylic acid with a thiazole derivative. The synthesized ligand was characterized by ^{1}H NMR and ^{13}C NMR, IR spectroscopic and mass spectrometry. The UV-visible spectrum accompanied with fluorescent spectral studies, binding constants and limit of detection proved efficient sensing abilities. The ligand was found to bind with one equivalent of an M^{2+} ion as validated by Job's plot and binding parameters. The novel fluorescent probe based on amide ligand exhibits precise and selective response to Mg^{2+} and Ni^{2+} ions in HEPES buffer solution showing the detection limit to be 2.1502×10^{-8} mol/L and 4.8007×10^{-8} mol/L, respectively. The binding stoichiometry of amide ligand with Mg^{2+} and Ni^{2+} was estimated by Job's plot method and found to be 1:1, which is further confirmed by mass spectrometry.

Keywords: Fluorescence quenching, Chemosensor, Binding constant, Metal ions detection Mg^{2+} and Ni^{2+}.

INTRODUCTION

The design and structure of molecules that exhibit fluorescence are the most important areas in the current research field for developing new sensor materials for various metal ions [1-3]. Pyridine 2,6-dicarboxamide based scaffolds have been progressively used in innumerable research work for specifically targeted identification of various cations ($Fe^{2+/3+}$, Cu^{2+}, Zn^{2+} and Pd^{2+}) and also drugs like warfarin [4-9]. The pincer-cavity chemosensors have effectively used chelate based detection techniques [3].

Transition metal complexes of N^2,N^6-*bis*(4-phenyl thiazole-2-yl)pyridine 2,6-dicarboxamide hold great potential in application in catalysis. Magnesium ion (Mg^{2+}) is vital in many cellular functions, including proliferating cells, dying cells, enzyme-driven biological events, transmission regulation, genome strength and cell communication [10-12]. Mg^{2+} plays a role in roughly 300 enzymatic processes in cells. The amount of intracellular Mg^{2+} is thought to influence the metabolism of cells [13]. Hypomagnesemia has been associated with a number of chronic diseases including diabetes, high blood pressure, bone loss, metabolic syndrome, brain injury and chemotherapeutic efficacy. Compared to other illnesses, hypermagnesemia is less widespread, but it is connected with prolonged renal failure and can lead to heart failure in extreme cases [14, 15]. Thus, it is crucial to design an incredibly precise and responsive fluorescent sensor that can recognize Mg^{2+} without any interruption from different metal ions. Since, fluorescent-based chemosensors offer significant advantages over other types, moreover the fluorescence analysis are sensitive, cost-effective, easy to perform, real-time detection and adaptable [16]. Sensing materials for detecting Mg^{2+} in aqueous solutions are limited, making it necessary to develop a novel sensor with good selectivity. On the other hand, Mg^{2+} sensors are very beneficial for quantifiable Mg^{2+} differentiation in water for consumption. Such Mg^{2+} sensors must be very selective to detect the analyte over other species. Men *et al.* [17] developed a fluorescent "turn-on" Mg^{2+} sensors that utilized an ordinary commercialized 3,5-dichloro salicylaldehyde (BCSA). Similarly, Wang *et al.* [18] developed a non-toxic, dual-functional chemosensor which detects Mg^{2+} and Zn^{2+} metal ions with limits of detection of 2.97×10^{-8} M and 3.07×10^{-7} M, respectively.

Nickel is also necessary for biological processes like oxygen consumption, metabolic processes and biosynthesis [19-21]. Nickel is mostly used in industrial applications to manufacture tools for chemical engineering. Nickel alloy has a variety of

industrial applications, including the fabrication of ornaments and other appliances [22,23]. Excessive nickel buildup can negatively impact mammalian respiratory and immunological systems, even though the relationship between nickel and mammalian health remains largely unexplored. Therefore, it is highly crucial to detect nickel ions. Over exposure to nickel can cause pulmonary fibrosis, renal illness and cardiovascular disease [24-26]. Numerous compounds have been synthesized to detect selectively nickel ions [27-34].

Recently, fluorescence quenching has gained popularity as a tool for studying various facets of ligand binding. Fluorescent detectors frequently show amplification for transition metal ions like Zn^{2+} [35,36], Cu^{2+} [37,38] and Fe^{3+} [39,40]. However, fluorescence compounds employed with conventional transition-metals fluorescent quenchers such as Ni^{2+} and Mg^{2+} are sparse. In this work, the ligand has been designed by the coupling of pyridine 2,6-dicarboxylic acid with 2-amino 4-phenyl thiazole containing appended thiazole ring. The thiazole ring is comparable to pyridine in terms of aromaticity and the field of chemistry but its electronic characteristics differ due to its weaker σ-donor and π-acceptor. The derived ligand's sensing abilities were investigated in three different solvents *viz*. CH_3OH (protic), THF (non-protic) and H_2O (HEPES buffer, 10 mM, pH = 7.2). The sensing material's ability to detect metal ions is facilitated by the chemical interactions that regulate the sensor bandgap. For instance, a bathochromic (red) shift results from decreasing the HOMO-LUMO energy gap, whereas a hypsochromic (blue) shift results from increasing it. This may help in the future creation of more potent fluorescent and colorimetric chemosensors for a range of uses including the commercial ones. The two metals ions Mg^{2+} and Ni^{2+} were found to show good fluorescent results.

EXPERIMENTAL

Pyridine-2,6-dicarboxylic acid and 2-amino-4-phenyl thiazole were purchased from Sigma-Aldrich, USA. The instrument AB-Sciex-Q-Star-LCMS-MS spectrometer was utilized for electrospray ionization mass analysis of the complexes. The ^1H NMR and ^{13}C NMR spectra of ligand were collected employing Bruker Advance 300 spectrometers, with TMS as internal reference material and $CDCl_3$ as solvent. The fluorescent spectra were collected using an instrument FP-8250 spectrofluorometer with a 1 cm quartz path. The 1 mM of fluorescent sensor stock solution was prepared with THF solvent. The luminous intensity of the ligand solution varies depending on its concentration. The optimal ligand concentration (60 μM) was determined for saturation. The 2.5 mM of metal ion stock solution was prepared by mixing chloride, acetate and nitrate salts in methanol solvent. The spectra were obtained at 318 nm, with a 5 nm excitation and emission slit. The fluorescent titration experiments were recorded using a fluorescent sensor at 60 μM with different concentration of Mg^{2+} and Ni^{2+} ions.

Synthesis of ligand: A reaction mixture containing pyridine-2,6-dicarboxylic acid (0.668 g, 0.0039 mol) and 2-amino-4 phenyl thiazole (1.40 g, 0.0079 mol) dissolved in 15 mL of pyridine was refluxed for 30 min at 120 ºC while stirring. Triphenyl phosphite (2.604 g, 0.00839 mol) was added dropwise to the resultant mixture and agitated at 100 ºC for another 6 h. Then, the solution was permitted to cool to ambient temperature before being immersed in ice water resulting in the formation of pale-yellow precipitate. The final product was purified, washed with water and air-dried (**Scheme-I**). Yield: 1.45 g (90%); m.p.: 265 ºC. Anal. calcd. (found) % for $C_{25}H_{17}N_5O_2S_2$: C, 62.10 (61.95); H, 3.54 (3.50); N, 14.48 (14.43); O, 6.62 (6.60); S, 13.26 (13.20). MS (ESI+ CH_3CN) *m/z*: 483.08; Found: 484.91 M^+. FT-IR (ATR, cm^{-1}): 3356 (N-H), 1684 (C=O). ^1H NMR (400 MHz, $CDCl_3$): 8.46 (q, *J* = 3.8 Hz, 1H), 8.16 (q, *J* = 7.92 Hz, 1H), 7.38 (d, *J* = 3.6 Hz, 1H), 7.62 (d, *J* = 4.58 Hz, 1H), 7.39 (t, *J* = 3.57 Hz, 1H), 6.99 (d, *J* = 1.84, 1H), 6.85 (d, *J* = 3.5 Hz, 1H), 13.12 (broad, NH); ^{13}C NMR (126 MHz, $CDCl_3$): 168.73, 165.42, 162.49, 157.86, 150.42, 150.11, 147.67, 146.72, 141.08, 135.48, 134.76, 129.32, 128.47, 127.68, 127.06, 126.42, 126.07, 119.34, 115.78, 109.66, 102.02.

Synthesis of metal complex: [{L}Cu(CH_3COO)]. A 10 mL of above synthesized ligand (0.241 g, 0.0005 mmol) dissolved in THF solution was added to a solution of [$Cu(CH_3COO)_2$] (0.090 g, 0.0005 mmol) prepared in 10 mL methanol with constant stirring. The consequent solution was subsequently agitated for 2 h. The resulting mixture was filtered and then the filtrate was left to evaporate. A greenish-blue crystalline solid was appeared after 10 h (**Scheme-II**). The coloured product was washed thoroughly from diethyl ether and dried under vacuum. Yield: 0.23 g (85%) m.p.: 270 ºC, FT-IR (ATR, cm^{-1}): 1607 (C=O). MS (ESI+ methanol, *m/z*): 558.52.

Preparation of solutions: In methanol, the stock solutions (2.5 mM) of Cu^{2+}, Ni^{2+}, Ag^+, Co^{3+}, Cd^{2+}, Pb^{2+}, Mn^{2+}, Pd^{2+}, Zn^{2+}, Mg^{2+}, Hg^{2+} and Fe^{3+} were prepared while that of ligand (1 mM) was prepared in THF solvent. The UV-visible and fluorescent

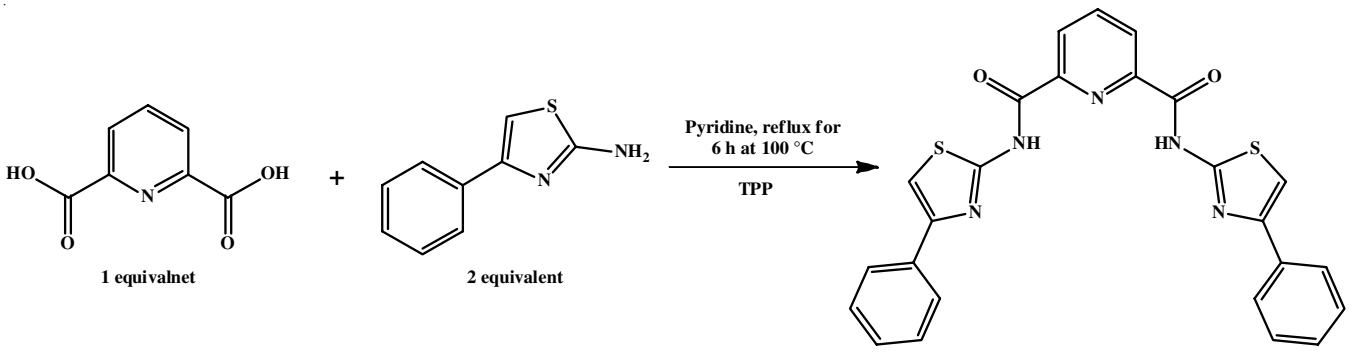

Scheme-I: Synthesis of ligand 1

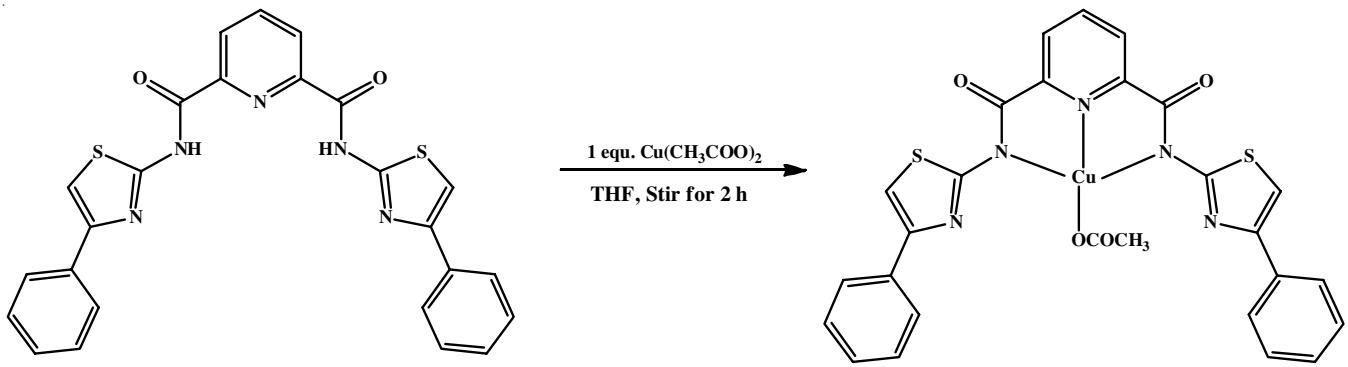

Scheme-II: Synthesis of metal complex

spectra were obtained at room temperature in a methanol/H_2O solution (pH 7.4, HEPES buffer, 0.2 mM). The fluorescence spectra were acquired using a 318 nm excitation wavelength (slit width: 5 nm/5 nm).

RESULTS AND DISCUSSION

^{1}H NMR studies: The ^{1}H NMR spectrum indicated a broad singlet for NH at δ 13.12 ppm (Fig. 1a). Furthermore, the predicted coupling between protons is also observable. In ^{13}C NMR spectra, the C=O carbon signal was detected at δ 162.49 ppm. In the pyridine-ringed carbon peaks have been identified at 141.08 ppm (1C), 127.68 ppm (2C) and 150.42 ppm (3C). On the other side, the thiazole carbon peaks were detected at 165.08 ppm (5C), 135.48 ppm (6C), 157.86 ppm (7C) and (10C) at 115.78 ppm (Fig. 1b).

Electronic and mass spectra: The spectrum of absorption of the ligand H_2L indicates λ_{max} at 318 (Fig. 2a). The λ_{max} attributed π-π* transition in the ligand molecule. Complex **1** exhibits a bathochromic shift and λ_{max} at 320 (Fig. 2b). The approximate mass of the ligand is *m/z* = 484.91 (Fig. 3).

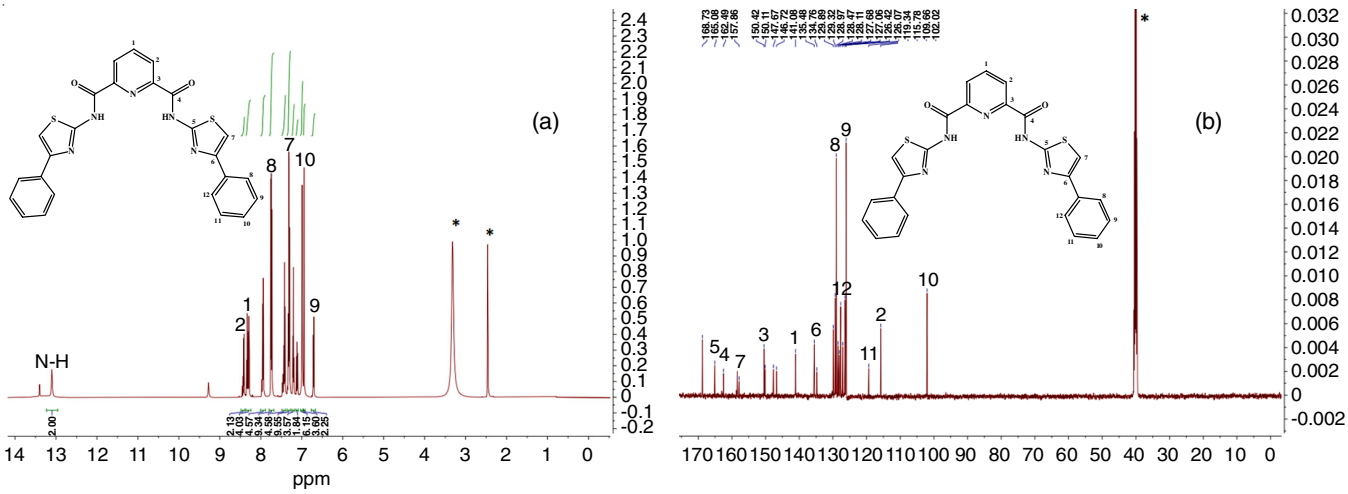

Fig. 1. (a) ^{1}H NMR and (b) ^{13}C NMR spectra of ligand, pyridine-2,6-dicarboxamide

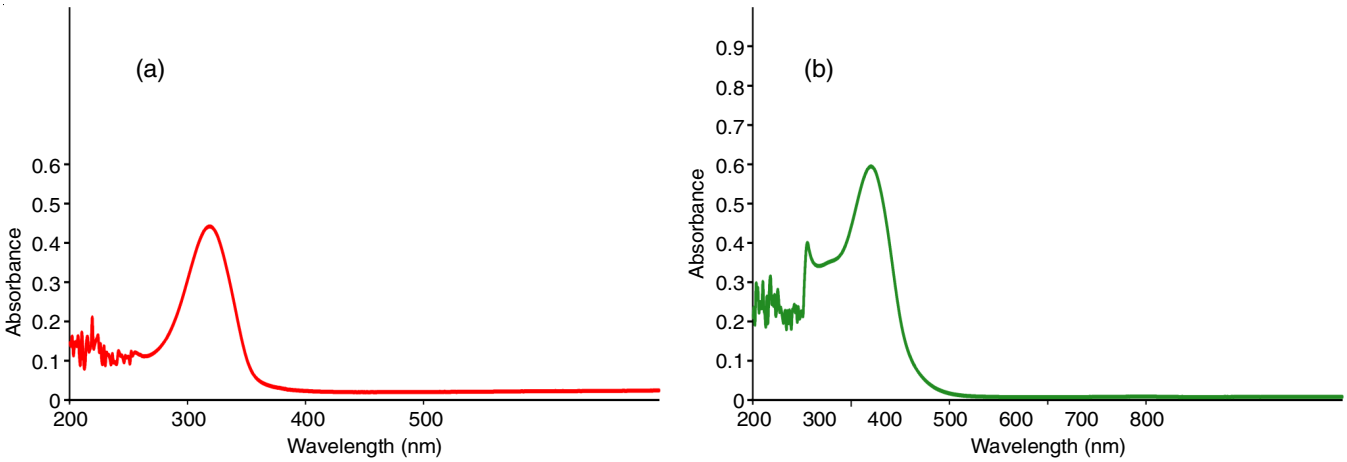

Fig. 2. UV-visible absorption spectra of ligand (a) and its complex (b)

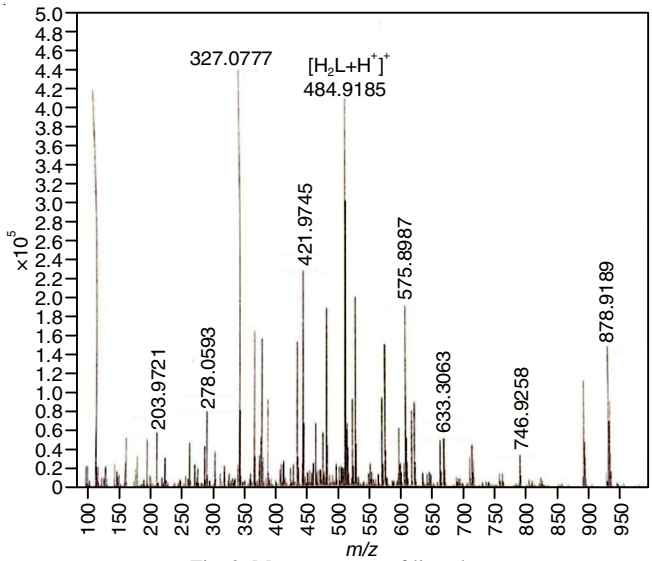

Fig. 3. Mass spectrum of ligand

IR spectra: In the IR spectra of ligand, the NH and CO stretching peaks associated with the amide linkages were observed at 3356 and 1684 cm^{-1}, respectively (Fig. 4). The metal complex was formed by combining the deprotonated ligands with an equivalent of the appropriate copper salt in the THF medium. In the FT-IR spectrum of complex, a broad peak at 3438 cm^{-1} is attributed to the ν(N-H) of the protonated heterocyclic ring. The disappearance of the NH *str.* band indicated that the amide group is deprotonated in contrast with the free ligand. These changes indicate the involvement of the anionic N-amide bonding in the coordination. The metal complex also exhibited a C=O stretching frequency at 1607 cm^{-1}, indicating a red shift of the band by 80-50 cm^{-1} compared to the ligand, which suggests that the amidic moieties in the complex are deprotonated.

Fluorescent spectral studies: The fluorescence sensing ability of the ligand towards various cations *viz*. Cu^{2+}, Ni^{2+}, Ag^{+}, Co^{3+}, Cd^{2+}, Pb^{2+}, Mn^{2+}, Pd^{2+}, Zn^{2+}, Mg^{2+}, Hg^{2+} and Fe^{3+} ions were investigated. The concentration of the ligand is determined by raising it from 20 µm to 60 µm, where it exhibits the highest fluorescence intensity. The ligand concentration required for the maximal intensity was 60 µm. The ligand's intensity varies with different metal ions and salt solutions. When various metal ions started to be added into the ligand solution, only Mg^{2+} and Ni^{2+} ions showed a significant shift in the intensity of fluorescence in compared to the ligand and other metal ions (Fig. 5).

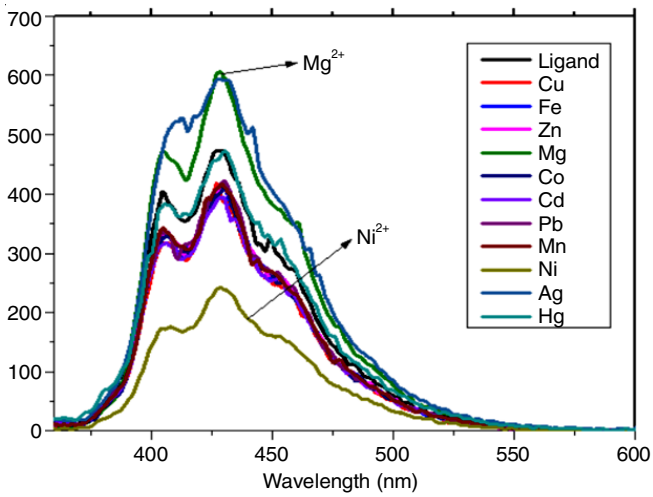

Fig. 5. Emission spectra of ligand in HEPES buffer and interaction with metal

The efficacy of ligand quenching can be examined using the Stern-Volmer plot. Using the Stern-Volmer plot, the binding constants were $2.04 \times 10^3\ M^{-1}$ and $2.97 \times 10^3\ M^{-1}$ respectively for Mg^{2+} and Ni^{2+}. The data shows that ligand has a detection limit of 2.1502×10^{-8} mol/L for Mg^{2+} and 4.8007×10^{-8} mol/L for Ni^{2+}. The ligand's fluorescence intensity was examined by gradually increasing Mg^{2+} and Ni^{2+} resulting in the quantitative quenching (Fig. 6).

Detection of Mg^{2+} and Ni^{2+}: Several metal ions were introduced into the ligand solution to examine its fluorescence sensing capacity. Fluorescent emissions from Mg^{2+} and Ni^{2+} ions

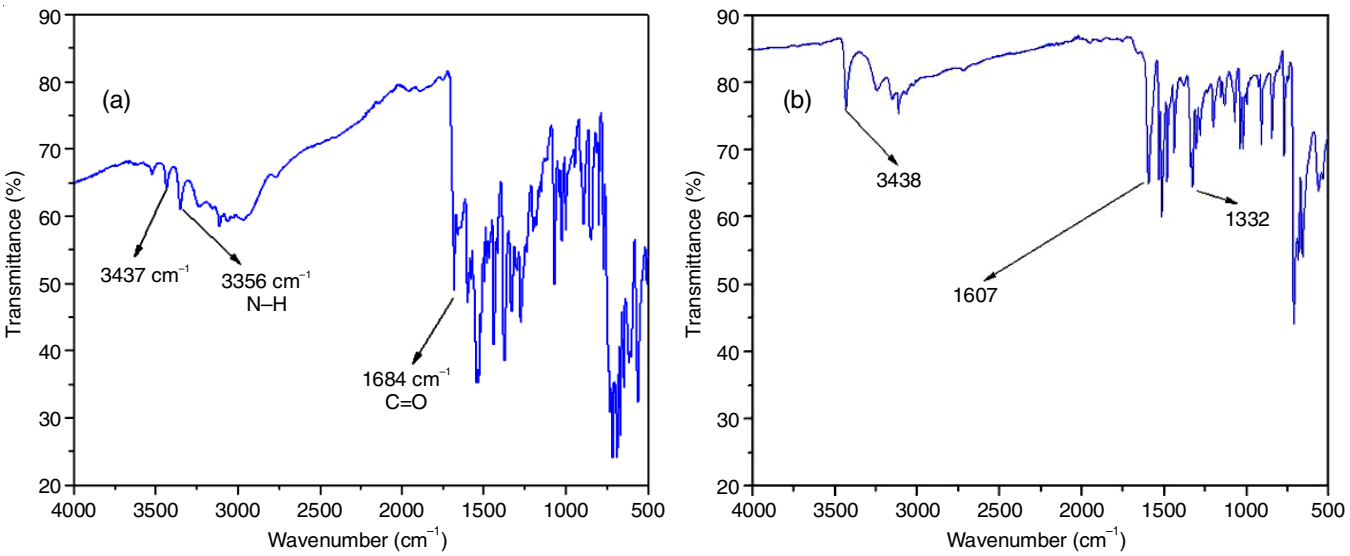

Fig. 4. FTIR spectra of ligand (a) and its complex (b)

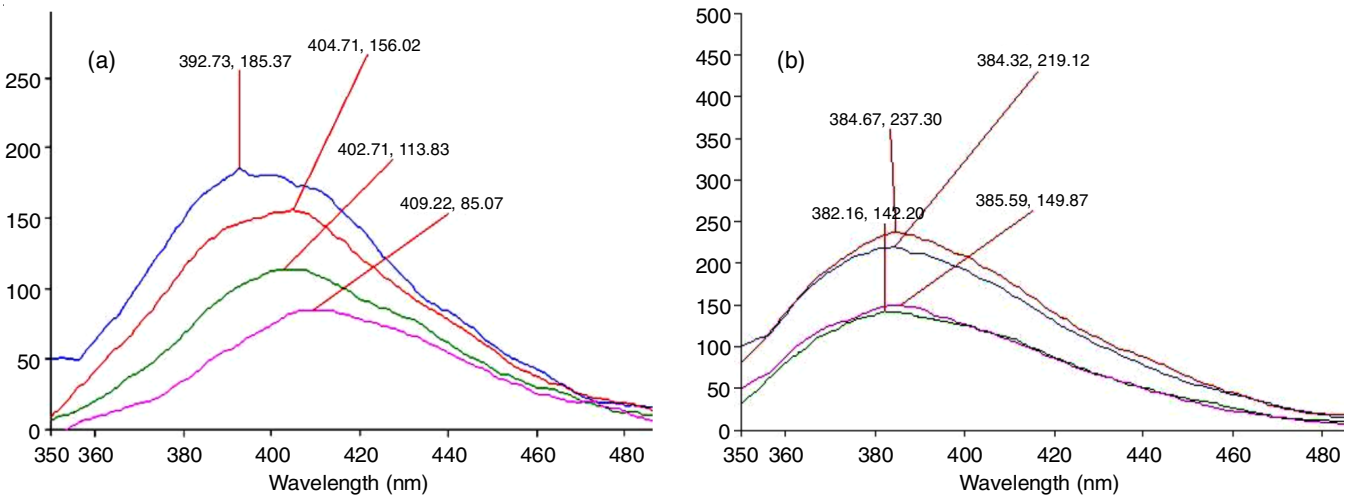

Fig. 6. Fluorescent spectra of chemosensor with variable concentration of (a) Mg^{2+} ion and (b) Ni^{2+} ion

at different concentrations are detected by the fluorescent sensor, while the intensity of emissions from other metal ions is almost identical to that of the ligand. Since the Mg^{2+} ions have a different binding affinity than other metal ions, they are utilized in the subsequent experiments.

Estimation of binding parameters: The spectral UV-visible titrations were used to calculate binding factors for Mg^{2+} and Ni^{2+} ions in three different solvents (CH_3OH, THF and HEPES buffers). Using eqn. 1, the binding constants (K_b) were determined using the Benesi-Hildebrand plot [4], whereas the limit of detection was determined using eqn. 2 [41].

$$\frac{1}{(I-I_0)} = \frac{1}{\{K_b(I_0-I_{min})[M^{2+}]\}} + \frac{1}{(I_0-I_{min})} \quad (1)$$

where I_0 and I are the absorption intensities of H_2L in both the absence and the presence of Mg^{2+} or Ni^{2+} ions.

$$\text{Detection limit} = \frac{3\sigma}{k} \quad (2)$$

where σ is the average deviation of ten blank replicated absorbance observations and k is the slope for absorbance *versus* the M^{2+} ion concentration plot.

The Job's plot uses a 1:1 stoichiometry and a continual fluctuation of mole fractions of Mg^{2+} and Ni^{2+} ions. The Benesi-Hildebrand plot confirmed the 1:1 stoichiometry of ligand and metal ions. Furthermore, the binding constants was found to be $2.04 \times 10^3\ M^{-1}$ and $2.97 \times 10^3\ M^{-1}$ for Mg^{2+} and Ni^{2+} ions, respectively.

Conclusion

A new fluorescent chemosensor (N^2,N^6-*bis*(4-phenyl thiazol-2-yl)pyridine-2,6-dicarboxamide) was developed and characterized through physicochemical and spectroscopic techniques. The efficacy of the fluorescent chemosensor to detect Mg^{2+} and Ni^{2+} ions among other metal ions for example, Mg^{2+}, Ag^+, Fe^{2+}, Na^+, K^+, Cu^{2+}, Ni^{2+}, Hg^{2+}, Pb^{2+}, Mn^{2+}, Pd^{2+}, Cd^{2+} and Mn^{3+} was successfully investigated. The fluorescent chemosensor for Mg^{2+} and Ni^{2+} ions has selectivity and detection limits at 2.1502×10^{-8} mol/L and 4.8007×10^{-8} mol/L, respectively.

ACKNOWLEDGEMENTS

This research work is funded by Council of Science and Technology, Lucknow Uttar Pradesh, India (Ref. CST/D/1253). One of the authors, NPS is thankful to Dr Ambedkar Center for Biomedical Research, Delhi University, Delhi for providing the spectral data and SAIF Punjab University, Chandigarh for ^1H NMR spectral analysis. The authors also thank the administrators of D.D.U. Gorakhpur University, Gorakhpur, India for providing the research facilities.

CONFLICT OF INTEREST

The authors declare that there is no conflict of interests regarding the publication of this article.

REFERENCES

1. K.P. Carter, A.M. Young and A.E. Palmer, *Chem. Rev.*, **114**, 4564 (2014); https://doi.org/10.1021/cr400546e
2. J. Lian, Q. Xu, Y. Wang and F. Meng, *Front. Chem.*, **8**, 593291 (2020); https://doi.org/10.3389/fchem.2020.593291
3. Y. Shi, W. Zhang, Y. Xue and J. Zhang, *Chemosensors*, **11**, 226 (2023); https://doi.org/10.3390/chemosensors11040226
4. D. Bansal and R. Gupta, *Dalton Trans.*, **45**, 502 (2016); https://doi.org/10.1039/C5DT03669K
5. P. Kumar, V. Kumar and R. Gupta, *RSC Adv.*, **5**, 97874 (2015); https://doi.org/10.1039/C5RA20760F
6. P. Kumar, V. Kumar and R. Gupta, *RSC Adv.*, **7**, 7734 (2017); https://doi.org/10.1039/C6RA27565F
7. V. Kumar, P. Kumar and R. Gupta, *RSC Adv.*, **7**, 23127 (2017); https://doi.org/10.1039/C7RA01453H
8. P. Kumar, V. Kumar and R. Gupta, *Dalton Trans.*, **46**, 10205 (2017); https://doi.org/10.1039/C7DT01811H
9. P. Kumar, V. Kumar, S. Pandey and R. Gupta, *Dalton Trans.*, **47**, 9536 (2018); https://doi.org/10.1039/C8DT01351A
10. H. Rubin, *BioEssays*, **27**, 311 (2005); https://doi.org/10.1002/bies.20183
11. A.A. Mushegian, *Sci. Signal.*, **9**, ec269 (2016); https://doi.org/10.1126/scisignal.aal3828
12. M.H. Pontes, J. Yeom and E.A. Groisman, *Mol. Cell*, **64**, 480 (2016); https://doi.org/10.1016/j.molcel.2016.05.008
13. B. O'Rourke, P.H. Backx and E. Marban, *Science*, **257**, 245 (1992); https://doi.org/10.1126/science.1321495
14. F. Wolf, *Mol. Aspects Med.*, **24**, 3 (2003); https://doi.org/10.1016/S0098-2997(02)00087-0

15. W. Jahnen-Dechent and M. Ketteler, *Clin. Kidney J.*, **5(Suppl 1)**, i3 (2012); https://doi.org/10.1093/ndtplus/sfr163
16. J. Kim, T. Morozumi and H. Nakamura, *Org. Lett.*, **9**, 4419 (2007); https://doi.org/10.1021/ol701976x
17. G. Men, C. Chen, S. Zhang, C. Liang, Y. Wang, M. Deng, H. Shang, B. Yang and S. Jiang, *Dalton Trans.*, **44**, 2755 (2015); https://doi.org/10.1039/C4DT03068K
18. Y. Wang, Z.-G. Wang, X.-Q. Song, Q. Chen, H. Tian, C.-Z. Xie, Q.-Z. Li and J.-Y. Xu, *Analyst*, **144**, 4024 (2019); https://doi.org/10.1039/C9AN00583H
19. S.B. Mulrooney and R.P. Hausinger, *Microbiol. Rev.*, **27**, 239 (2003); https://doi.org/10.1016/S0168-6445(03)00042-1
20. S.W. Ragsdale, *J. Biol. Chem.*, **284**, 18571 (2009); https://doi.org/10.1074/jbc.R900020200
21. R.J. Maier, *Biochem. Soc. Trans.*, **33**, 83 (2005); https://doi.org/10.1042/BST0330083
22. K.S. Kasprzak, F.W. Sunderman and K. Salnikowa, *Mutat. Res.*, **533**, 67 (2003); https://doi.org/10.1016/j.mrfmmm.2003.08.021
23. P.H. Kuck, Mineral Commodity Summaries: Nickel, United States Geological Survey (2006).
24. X.Q. Liu, X. Zhou, X. Shu and J. Zhu, *Macromolecules*, **42**, 7634 (2009); https://doi.org/10.1021/ma901879t
25. J.R. Sheng, F. Feng, Y. Qiang, F.G. Liang, L. Sen and F.-H. Wei, *Anal. Lett.*, **41**, 2203 (2008); https://doi.org/10.1080/00032710802237673
26. H.X. Wang, D.L. Wang, Q. Wang, X. Li and C.A. Schalley, *Org. Biomol. Chem.*, **8**, 1017 (2010); https://doi.org/10.1039/b921342b
27. B. Qin, X. Zhang and J. Zhang, *Cryst. Growth Des.*, **20**, 5120 (2020); https://doi.org/10.1021/acs.cgd.0c00308
28. M. Shamsipur, T. Poursaberi, A.R. Karami, M. Hosseini, A. Momeni, N. Alizadeh, M. Yousefi and M.R. Ganjali, *Anal. Chim. Acta*, **501**, 55 (2004); https://doi.org/10.1016/j.aca.2003.09.008
29. V.K. Gupta, R.N. Goyal, S. Agarwal, P. Kumar and N. Bachheti, *Talanta*, **71**, 795 (2007); https://doi.org/10.1016/j.talanta.2006.05.036
30. I. Grabchev, J.M. Chovelon and X. Qian, *New J. Chem.*, **27**, 337 (2003); https://doi.org/10.1039/b204727f
31. I. Qureshi, M.A. Qazi and S. Memon, *Sens. Actuators B Chem.*, **141**, 45 (2009); https://doi.org/10.1016/j.snb.2009.06.010
32. H. Li, S.J. Zhang, C.L. Gong, Y.-F. Li, Y. Liang, Z.-G. Qi and S. Chen, *Analyst*, **138**, 7090 (2013); https://doi.org/10.1039/c3an01162c
33. S. Goswami, S. Chakraborty, S. Paul, S. Halder and A.C. Maity, *Tetrahedron Lett.*, **54**, 5075 (2013); https://doi.org/10.1016/j.tetlet.2013.07.051
34. L. Lin, S. Hu, Y. Yan, D.-J. Wang, L. Fan, Y.-J. Hu and G.-D. Yin, *Res. Chem. Intermed.*, **43**, 283 (2017); https://doi.org/10.1007/s11164-016-2621-9
35. S. Atilgan, T. Ozdemir and E.U. Akkaya, *Org. Lett.*, **10**, 4065 (2008); https://doi.org/10.1021/ol801554t
36. P. Teolato, E. Rampazzo, M. Arduini, F. Mancin, P. Tecilla and U. Tonellato, *Chem. Eur. J.*, **13**, 2238 (2007); https://doi.org/10.1002/chem.200600624
37. H.J. Kim, J. Hong, A. Hong, S. Ham, J.H. Lee and S.J. Kim, *Org. Lett.*, **10**, 1963 (2008); https://doi.org/10.1021/ol800475d
38. R. Martinez, F. Zapata, A. Caballero, A. Espinosa, A. Tarraga and P. Molina, *Org. Lett.*, **8**, 3235 (2006); https://doi.org/10.1021/ol0610791
39. N.C. Lim, S.V. Pavlova and C. Bruckner, *Inorg. Chem.*, **48**, 1173 (2009); https://doi.org/10.1021/ic801322x
40. J.L. Bricks, A. Kovalchuk, C. Trieflinger, M. Nofz, M. Buschel, A.I. Tolmachev, J. Daub and K.J.J. Rurack, *J. Am. Chem. Soc.*, **127**, 13522 (2005); https://doi.org/10.1021/ja050652t
41. C. Liang, W. Bu, C. Li, G. Men, M. Deng, Y. Jiangyao, H. Sun and S. Jiang, *Dalton Trans.*, **44**, 11352 (2015); https://doi.org/10.1039/C5DT00689A